Image Guidance for Robot-Assisted Ankle Fracture Repair

Anthony Wu, Jayaram Mandavilli, Asef Islam

Mentors: Dr. Jeff Siewerdsen and Dr. Wojtek Zbijewski

February 25, 2020

Computer Integrated Surgery II

Dr. Russ Taylor

Spring 2020

Johns Hopkins University, Baltimore, MD

1. Introduction:

Summary

This project concerns developing and validating an image guidance framework for application to robotic-assisted fibular reduction in ankle fracture surgery. The aim is to produce and demonstrate proper functioning of a software for automatic determination of directions for fibular repositioning with the ultimate goal of application to a robotic reduction procedure that can reduce the time and complexity of the procedure as well as provide the benefits of reduced error in ideal final fibular position, improved syndesmosis restoration and reduced incidence of post-traumatic osteoarthritis. The focus of this product will be developing and testing the image guidance software, from input of preoperative images through the steps of automated segmentation and registration until output of a final transformation that can be used as instructions to a robot on how to reposition the fibula, but will not involve developing or implementing the hardware of the robot itself.

Background

Ankle fractures occur with a frequency of around 174 cases per 100,000 adults per year, with over 5 million yearly cases in the U.S. alone (Goost et al), affecting mainly young active people and the elderly. Ankle fractures most commonly involve a fracture in the lower fibula which can also result in disruption of the syndesmosis, or the alignment of other bones and ligaments within the ankle joint, if the fibula is displaced. This is due to the displacement of the lower fibula causing damage and forceful shifting of these ligaments and other connective tissue. This can lead to many long-term complications including post-traumatic osteoarthritis (PTOA) if the proper syndesmosis is not restored.

Figure 1: Healthy ankle (left) and ankle after fracture (middle) with fibular fracture and displacement of lower fibula in ankle joint, along with post-treatment ankle (right) with fixed fracture and restored fibula position.

The proximal fracture can be treated with relatively little difficulty such as by fixation with metal screws. However, the second part of the surgery is fibular reduction, or movement of the lower fibula back into proper position to reconstruct the joint and restore syndesmosis. The current standard of care for this procedure is visual estimation by the surgeon to determine where to place the fibula and screw-based fixation of syndesmosis. In one study over 20% of patients who underwent reduction via this method were shown through CT scans shortly

afterwards to have syndesmotic malreduction, which was defined as a greater than 2 mm widening of syndesmosis compared to the patient's other, healthy ankle (Nagvi et al). The most common reason for re-operation in the weeks immediately following the initial ankle fracture surgery is syndesmotic malreduction (Ovaska et al). Furthermore, the incidence of PTOA in ankle fracture patients is as high as 70% (Mehta et al). Evidently, the standard of care for reduction is inadequate for proper syndesmotic restoration and prevention of PTOA.

2. Technical Approach:

Steps in Approach:

1. **Automated Segmentation**

The first step in an image-guided approach is fast, automated segmentation of the pre-operative images in order to identify and save the relevant anatomical features, in this case the fibula and other bones of the ankle. A promising existing approach to automated segmentation is active shape models (ASMs) (Brehler et al). An ASM model is trained by taking in as input a training set of several segmentations of a single bone from different patients and then performing a PCA-based analysis to identify and characterize the principal modes of variation in the surface morphology of the bone within the population of training samples. The model comprises a set of basis functions for each principal component of variation, which can be tuned and create a deformable template that can be mapped onto any new example by minimizing residuals. Thus, this can be applied to automated segmentation by using this template object in order to map onto a new image and segment the bone given some initialization.

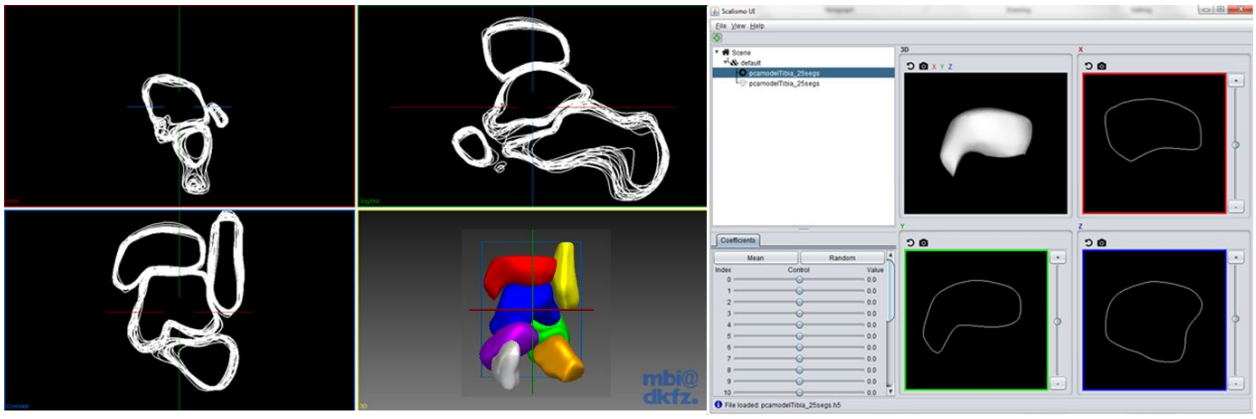

Figure 2: Example of multiple registered 3D CT segmentations of ankle bones (left) which are used to construct ASM (right).

ASMs can be improved even further by updating them to Coupled Active Shape Models (cASMs). Traditional ASMs are trained independently for individual bones and separately initialized, however as a result they are susceptible to errors in the narrow articular joint spaces between bones if there is poor contrast in the image and can result in producing segmentations with overlap in adjacent bones. cASMS are trained with consideration of multiple bones simultaneously and incorporate the spatial relations and articular joint widths between adjacent bones as features as well, and thus they are able to improve on the accuracy of segmentation within these joint spaces and prevent overlaps.

While in this work the cASMs were evaluated in high-resolution cone-beam CT (CBCT) images, they have not yet been tested in pre-operative C-arm images for 2D-3D reconstruction. Thus, an important step in adopting the cASM approach for this project will be to evaluate its accuracy in segmenting C-arm images and improving it to do so, including improving the initializations and adding corrections for noise and artifacts.

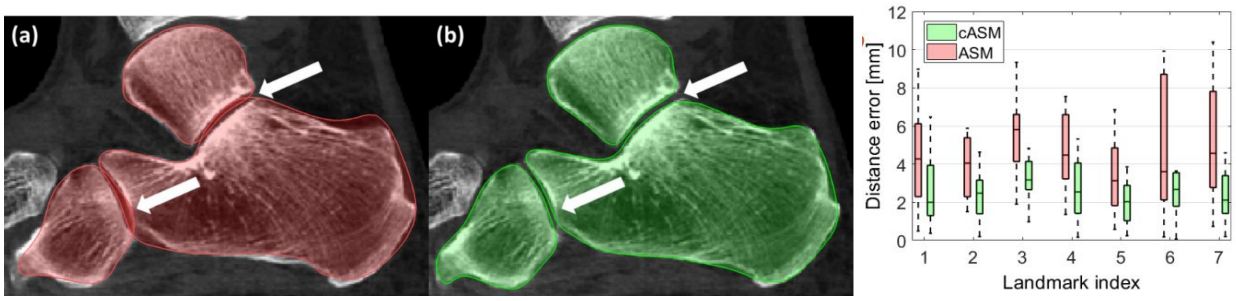

Figure 3: Comparison of traditional ASMs (red) and cASMs (green) showing reduced overlap and error in segmentations within articular joint spaces as well as reduced error in landmark positions.

A deep learning approach will also be taken, as it is likely that the ASM model will not provide sufficient segmentation accuracy. It will be used to also conduct image segmentation, like the ASM. The purpose of this is to build this model to hopefully get a higher segmentation accuracy than the ASM model. The final approach chosen will be the one that yields the highest accuracy. It is possible that the final model chosen is a combination of the ASM and the neural network. The plan for the deep neural network is to utilize a convolutional neural network (CNN). These are commonly used for image processing in a lot of domains. The specifics of the neural network are currently unknown. However, there are some major characteristics that will most likely be implemented. Maximum pooling will most likely be used over average pooling as it is known to be more effective in image classification. This is because this technique focuses on the most important characteristics in the image. This is helpful in classification because it does not let other, less significant, pixels affect the classification and only looks at what is really important. Pooling is also beneficial because it is able to focus on what is really important. This reduces the computational burden of training the neural net. Other techniques such as dropout. Another strategy that could be used is increasing the number of epochs. This will need to be carefully managed because if intraoperative c-arm data is being utilized, the segmentation will need to be determined quickly. The model will need to be fine-tuned, which will be an ongoing process. The goal is to achieve high accuracy, the exact accuracy goals for the deep learning model can be seen in the deliverables section.

Whichever final approach is used for automated segmentation, it would be used to automatically segment the ankle bones of both of the patient's ankles (the healthy one and the injured one). The model, or combination of models, which yields the highest segmentation accuracy (as compared to manually segmented images through minimizing square residuals) will be used.

2. **Registration**

   After segmentation is completed, the instructions for reduction must be computed. This will be done by using the patient's healthy ankle as a guideline for how to reconstruct the

injured ankle. The segmentation of the healthy fibula will be mirrored and flipped, and then the rigid registration from the injured to the healthy ankle will be computed. The resulting calculated transformation will be used as instructions for the robot on how to position the injured fibula.

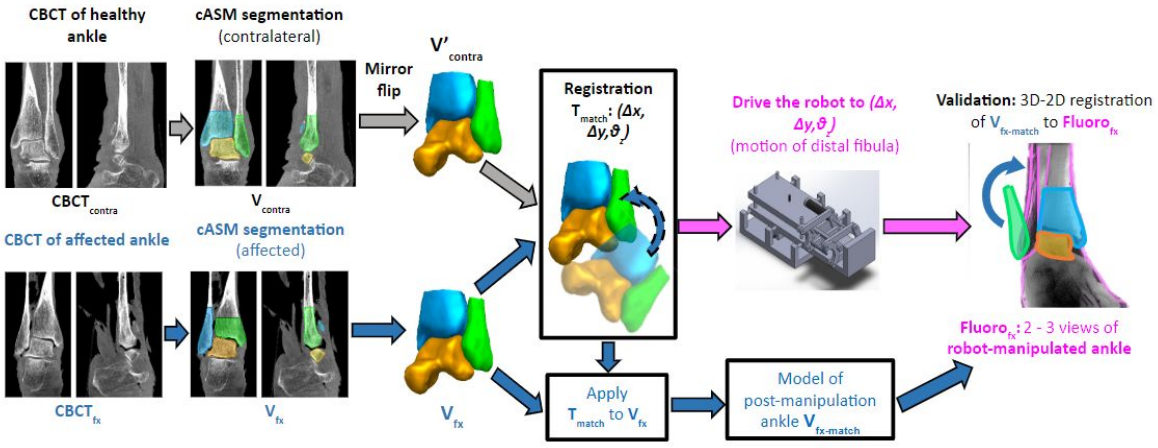

Figure 4: Outline of approach.

3. Project Plan:

Deliverables

- Minimum: (Expected by 3/11)
    - Working Adjust Active Shape Model
        - Our team will first segment healthy ankle C-arm images without metal artifacts. After consulting with mentors, our segmentation error for each bone should not exceed a mean of 5mm.
        - Our team will next segment healthy ankle C-arm images with metal artifacts. After consulting with mentors, our segmentation error for each bone should not exceed a mean of 5mm.
        - The purpose of this deliverable is to ensure that our ASM model is working correctly, which we plan to use as a layer of our neural network for the deep learning segmentation model.
    - Perform error analysis and show failure modes of ASM model
        - Our mentors do not expect the ASM model to perform adequately for C-arm images with metal artifacts. As a result, our team will create an analysis that documents why the ASM model cannot be implemented on its own.
- Expected: (Expected by 4/11)
    - Working Deep Learning Segmentation Model
        - Our team will first segment healthy ankle C-arm images with and without metal artifacts. After consulting with mentors, our segmentation error for each bone should improve to a mean of 2mm.

        - Our team will next apply our deep learning model to unhealthy ankle C-arm images with and without metal artifacts. After consulting with mentors, our segmentation error for each bone should not exceed a mean of 2mm.
- Maximum: (Expected by 5/6)
    - Conduct experiments on cadavers
        - We will first place multiple metal markers on the ankle, take an image, then disrupt the fibula, and then take another image.
        - Our team will apply our deep learning models from our expected deliverables on the unhealthy ankles.
        - We will next apply a deformable registration algorithm to transform the unhealthy ankle to the healthy ankle.
        - To determine the error, we will take the sum of the square residuals between the metal marker landmarks. After consulting with mentors, we expect this error to have a maximum mean of 2mm.
    - Combine the deep learning segmentation model with multi-body 3D-2D registration to guide reduction within a 1mm error
    - Written Paper

Dependencies

- **Feedback from Mentors**
    - Plan: Meet with mentors at med campus every Friday between 3:30pm and 5pm
    - Backup: Communicate via email and schedule meeting times outside of standard meeting times
    - Point of Contact: Dr. Siewerdsen and Dr. Zbijewski
    - Date Solved: 02/07/2020
- **Imaging Libraries**
    - Plan: Utilize already established MATLAB packages, such as Image Processing Toolbox, Computer Vision Toolbox, and Robotics System Toolbox
    - Backup: N/A
    - Point of Contact: N/A
    - Date Solved: 02/07/2020
- **Deep Learning Libraries**
    - Plan: Utilize already established Python packages (Tensorflow, PyTorch)
    - Backup: N/A
    - Point of Contact: N/A
    - Date Solved: 02/07/2020
- **Version Control**
    - Plan: Utilize GitHub to backup code
    - Backup: Use a backup hard drive
    - Point of Contact: N/A

    - Date Solved: 02/07/2020
- **Segmented C-Arm Images**
    - Plan: Segment already generated C-Arm data with iStar's segmentation software
    - Backup: Use C-arm provided by the lab to get data that can be segmented with segmentation software. This will require radiation training with Dr. Siewerdsen
    - Point of Contact: Dr. Qian Cao
    - Date Needed: 03/11/2020
- **Computers (GPU Array for Deep Learning)**
    - Plan: Connect to lab computers and GPU cluster from personal laptops
    - Backup: Go to medical campus to work directly on lab computers
    - Point of Contact: Dr. Siewerdsen
    - Date Needed: 03/11/2020
- **Validation Data**
    - Plan: Use Cadaver ankles at Carnegie as test
    - Backup: Use phantom model ankles
    - Point of Contact: Dr. Siewerdsen
    - Date Needed: 04/02/2020
- **C-Arm Mentoring**
    - Plan: Find member in iStar lab to help our team perform imaging on C-Arm
    - Backup: Obtain training of C-arm ourselves by performing online training
    - Point of Contact: Wojtek Zbijewski
    - Date Needed: 04/02/2020

Timeline

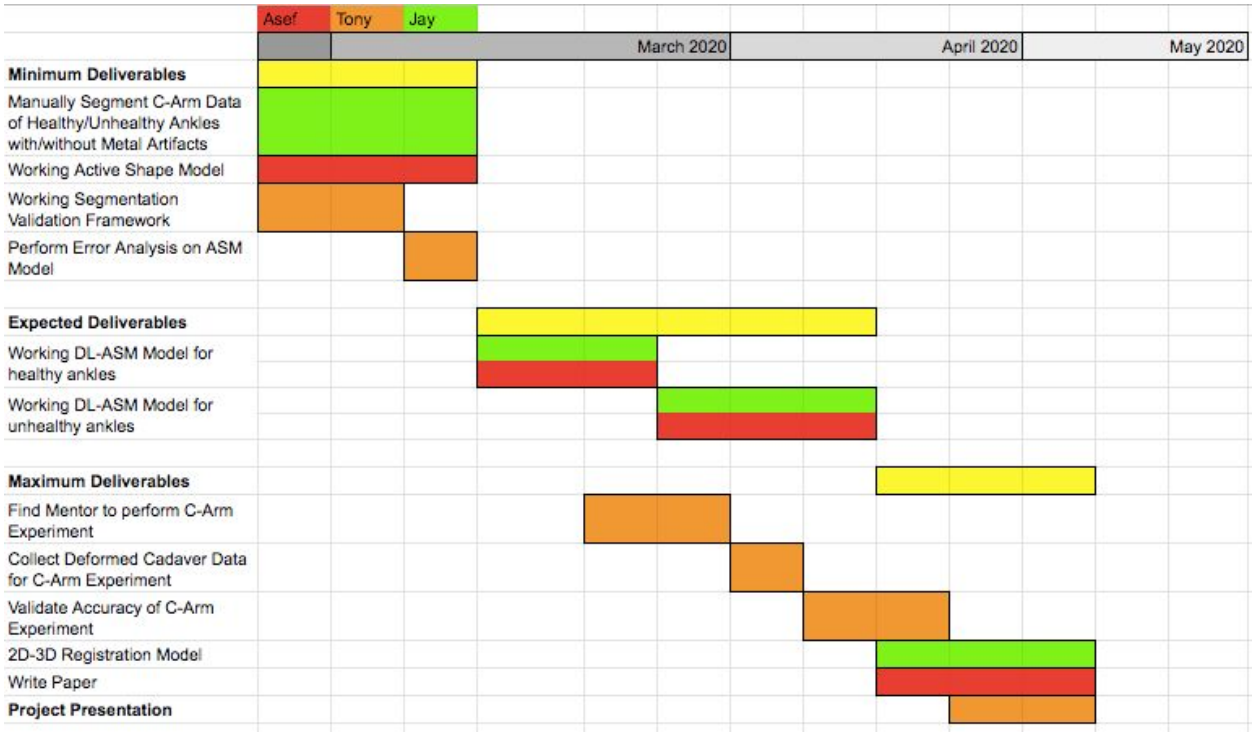

4. Acknowledgements

This project is supported by Dr. Jeff Siewerdsen and Wojtek Zbijewski of the JHMI I-STAR Lab. We would like to thank them for their continued support and enthusiasm.

5. References

M. Brehler, A. Islam, L. Vogelsang, D. Yang, W. Sehnert, D. Shakoor, S. Demehri, J. H. Siewerdsen, W. Zbijewski, "Coupled Active Shape Models for Automated Segmentation and Landmark Localization in High-Resolution CT of the Foot and Ankle"

Goost H, Wimmer MD, Barg A, Kabir K, Valderrabano V, Burger C. Fractures of the ankle joint: investigation and treatment options. *Dtsch Arztebl Int*. 2014;111(21):377–388. doi:10.3238/arztebl.2014.0377

Ovaska MT, Mäkinen TJ, Madanat R, Kiljunen V, Lindahl J. A comprehensive analysis of patients with malreduced ankle fractures undergoing re-operation. *Int Orthop*. 2014;38(1):83–88. doi:10.1007/s00264-013-2168-y

Naqvi, G. A., Cunningham, P., Lynch, B., Galvin, R., & Awan, N. (2012). Fixation of Ankle Syndesmotic Injuries: Comparison of TightRope Fixation and Syndesmotic Screw Fixation for Accuracy of Syndesmotic Reduction. *The American Journal of Sports Medicine*, *40*(12), 2828–2835. https://doi.org/10.1177/0363546512461480

Y. Otake, R. J. Murphy, R. B. Grupp, Y. Sato, R. H. Taylor, and M. Armand, "Comparison of Optimization Strategy and Similarity Metric in Atlas-to-subject Registration Using Statistical Deformation Model", in Proc. SPIE 9415, Medical Imaging 2015: Image-Guided Procedures, Robotic Interventions, and Modeling, San Francisco, 8-10 Feb., 2015. p. 94150Q. 10.1117/12.2081310

R. B. Grupp, M. Armand, and R. H. Taylor, "Patch-Based Image Similarity for Intraoperative 2D/3D Pelvis Registration During Periacetabular Osteotomy", in MICCAI Clinical Image-Based Procedures,, Grenada, Spain, September, 2018. pp. 153-163.

R. B. Grupp, R. A. Hegeman, R. J. Murphy, C. P. Alexander, Y. Otake, B. A. McArthur, M. Armand, and R. H. Taylor, "Pose Estimation of Periacetabular Osteotomy Fragments with Intraoperative X-Ray Navigation", IEEE Trans Biomed Eng., vol. 67- 2, pp. 441-452, Feb., 2020. Epub 8 March 2019 Epub 8 March 2019. 10.1109/TBME.2019.2915165

O. Sadowsky, G. Chintalapani, and R. H. Taylor, “Deformable 2D-3D Registration of the Pelvis with a Limited Field of View, Using Shape Statistics”, in MICCAI, Brisbane, Australia, 2007. pp. 519–526. PMID: 18044608

G. Chintalapani, O. Sadowsky, L. M. Ellingsen, J. L. Prince, and R. H. Taylor, “Integrating Statistical Models of Bone Density into Shape Based 2D-3D Registration Framework.”, in PMMIA: A workshop in Conjunction with MICCAI '09, London, 2009. pp. 151-161.

O. M. Ahmad, K. Ramamurthi, K. E. Wilson, K. Engelke, M. Bouxsein, and R. H. Taylor, “3D Structural Measurements of the Proximal Femur from 2D DXA Images Using a Statistical Atlas”, in SPIE Medical Imaging, Orlando, Florida, February, 2009. pp. 726005-726005-8. 10.1117/12.811176

X. Kang, M. Armand, Y. Otake, W.-P. Yau, P. Y. S. Cheung, Y. Hu, and R. H. Taylor, “Robustness and Accuracy of Feature-Based Single Image 2D-3D Registration without Correspondences for Image-Guided Intervention”, IEEE Trans Biomed Eng., vol. 61- 1, pp. 149-161, January, 2014. Aug 15, 2013 Aug 15, 2013.

X. Kang, W.-P. Yau, and R. H. Taylor, “Simultaneous Pose Estimation and Patient-Specific Model Reconstruction from Single Image Using Maximum Penalized Likelihood Estimation (MPLE)”, Pattern Recognition, vol. 57- C, pp. 61-69, Sept., 2016. 2 April 2016 2 April 2016. http://www.sciencedirect.com/science/article/pii/S0031320316300103 http://dx.doi.org/10.1016/j.patcog.2016.03.025